

Global Broadband IR Surface Emissivity Computed from Combined ASTER and MODIS Emissivity over Land (CAMEL)

Michelle Feltz, Eva Borbas, Robert Knuteson, Glynn Hulley*, Simon Hook*

University of Wisconsin-Madison Space Science and Engineering Center (SSEC)
Cooperative Institute for Meteorological Satellite Studies (CIMSS)
*California Institute of Technology Jet Propulsion Laboratory (JPL)

1. INTRODUCTION

Infrared surface emissivity is an important variable in the estimation of the surface longwave net energy balance, which is a critical parameter in Earth's radiation budget as well as weather and climate models. Surface emissivity, a measure of how closely Earth's surface acts as a blackbody in emitting radiation to the atmosphere, contains variations in the spectral domain based upon the surface composition and vegetation cover; thus, it will vary in space and time as surface cover and composition changes.

In various radiative transfer models, it is common practice to use a single, constant, global broadband surface emissivity value. This can lead to systematic biases in the estimated net radiation for any particular location and time of year. This practice was first initiated due to a lack of spatially and temporally varying global broadband emissivity (BBE) measurements. However, several efforts have recently been put forth to develop BBE datasets using satellite measurements (e.g. Wang et al. 2005; Tang et al. 2010; Ogawa et al. 2002, 2008; Huazhong et al. 2013; Cheng et al. 2012, 2015). Such methods have typically involved regressions of BBE to measured narrowband emissivities from satellite instruments such as the Moderate Resolution Imaging Spectroradiometer (MODIS), Advanced Spaceborne Thermal Emission and Reflection Radiometer (ASTER), or the Advanced Very High Resolution Radiometer (AVHRR). Parameterizations of BBE have been developed for input into models such as in Wilber et al. (1999), where BBE values are provided for different infrared bands and International Geosphere-Biosphere Programme (IGBP) land cover classifications.

Under the NASA Making Earth Science Data Records for Use in Research Environments (MEaSUREs) project, a new global, high spectral resolution land surface emissivity database is being made available as part of the Unified and Coherent Land Surface Temperature and Emissivity Earth System Data Record. This new database is created by a merging of the MODIS baseline-fit emissivity database (UWIREMIS) developed at the University of Wisconsin - Madison and the ASTER Global Emissivity Database produced at the California Institute of

Technology Jet Propulsion Laboratory (JPL). This new Combined ASTER and MODIS Emissivity over Land (CAMEL) database will be available for 2000 - 2017 at monthly mean, ~5 km resolution for 13 bands between 3.6-14.3 μm . Using a principal component regression approach, this dataset will be extended to 417 infrared spectral channels.

This work presents broadband emissivity calculated using a recently released beta version of the MEaSUREs CAMEL database, v0.6. Monthly, ~5 km resolution BBE is calculated over the globe for 2003-2015. BBE is computed over two wavelength ranges—the full available CAMEL spectrum of 3.6-14.3 μm and 8.0-13.5 μm , which has been determined to be an optimal range for computing the most representative all wavelength, longwave net radiation (Ogawa and Schmugge, 2004; Cheng et al., 2013). This dataset provides the advantages of being consistent with the MEaSUREs HSR emissivity and not requiring regression schemes—BBE can be calculated by simple numerical integration over the MEaSUREs high spectral resolution emissivity product. Statistics are calculated for IGBP land cover categories as well as for the Köppen-Geiger Climate Classification schemes. Monthly climatologies over the available years are presented.

2. DATA

This work uses the NASA MEaSUREs CAMEL beta v0.6 release over 2003 through 2015.

NASA's EOS MODIS instrument is used to provide monthly, global skin temperature and IGBP land cover classification on a 0.5x0.5 degree grid resolution. Specifically, the MOD11C3 skin temperature product is used which is made available online by the NASA and United States Geological Survey (USGS) Land Processes Distributed Active Archive Center at https://lpdaac.usgs.gov/dataset_discovery/modis. The land cover product MCD12Q1 is made available by the Global Land Cover Facility online at <http://glcf.umd.edu/data/lc/> and more information can be found in Channan et al. (2014).

Köppen-Geiger Climate Classification scheme data was accessed at <http://koeppen-geiger.wu-wien.ac.at/present.htm>. More information about this scheme can be found in Kottek et al. (2006).

3. METHODOLOGY

BBE is calculated by using the following equation (Cheng et al., 2013):

$$\varepsilon_{BB} = \frac{\int_{\lambda_1}^{\lambda_2} \varepsilon_{\lambda} B_{\lambda}(T_s) d\lambda}{\int_{\lambda_1}^{\lambda_2} B_{\lambda}(T_s) d\lambda} \quad (1)$$

where ε_{λ} is the MEaSURES monthly, high spectral resolution emissivity and B_{λ} is the Planck function at wavelength λ , and T_s is the monthly MODIS land surface temperature, specifically the average of the day and night. If no MODIS temperature is available a default value of 290 K is used. Studies have shown that BBE is insensitive to typical fluctuations of Earth's temperature. BBE is calculated for the following two wavelength ranges: 3.6-14.3 and 8.0-13.5 μm . Figure 1 shows example overlaid CAMEL emissivity spectra on the 13 channels as well as the 417 high spectral resolution channels for four test sites. A quality flag for BBE is also defined as seen in Table 1.

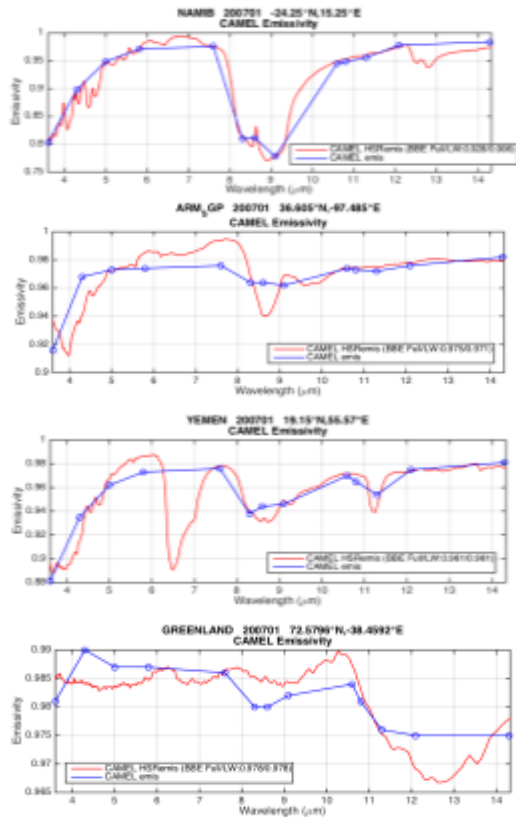


Figure 1a. Overlaid CAMEL emissivity for January 2007 on the 13 (blue) and 417 high spectral resolution (red) channels over the Namib Desert (top), Atmospheric Radiation Measurement Southern Great Plains (ARM SGP) site (second from top), Yemen (second from bottom), and Greenland (bottom).



Figure 1b. Land cover images from Google Maps (citation on images) over characteristic quartz of Namib Desert (top left), crop mosaic of ARM SGP site (top right), carbonate region in Yemen (bottom left), and Greenland snow/ice cover next to Summit Station (bottom right).

Table 1. CAMEL BBE Quality Flag Definition

BBE Quality Flag Definition	
0	Good – BBE btwn 0.8-1.0
1	Good – no MODIS data, 290 K used
2	BBE outside 0.8-1.0 range
3	BBE calculation failed
4	No BBE calc – no CAMEL coefficients available
5	No BBE calc – sea or inland water

4. RESULTS

4.1 CAMEL Broadband Emissivity

Fig 2 shows monthly, global, Jan 2007 BBE for both wavelength ranges. The wider 3.6-14.3 μm range BBE is larger, but qualitatively similar to the 8.0-13.5 μm range in spatial variation.

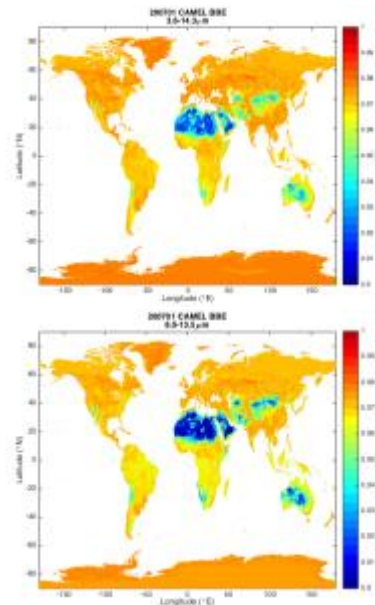


Figure 2. January 2007 monthly CAMEL BBE for 3.6-14.3 μm (top) and 8.0-13.5 μm (bottom).

As previously mentioned, broadband emissivity values used in some land surface or radiative models are set to a single, constant, global value over time and space. Fig 3 shows maps of 8.0-13.5 μm Jan 2007 BBE minus various example constants. While the figures support the use of a spatially varying BBE in modeling endeavors, they also show that if a single, constant value were to be used, that 0.97 or 0.975 rather than 0.98, which is used in some radiative models, is the optimal choice for a BBE constant.

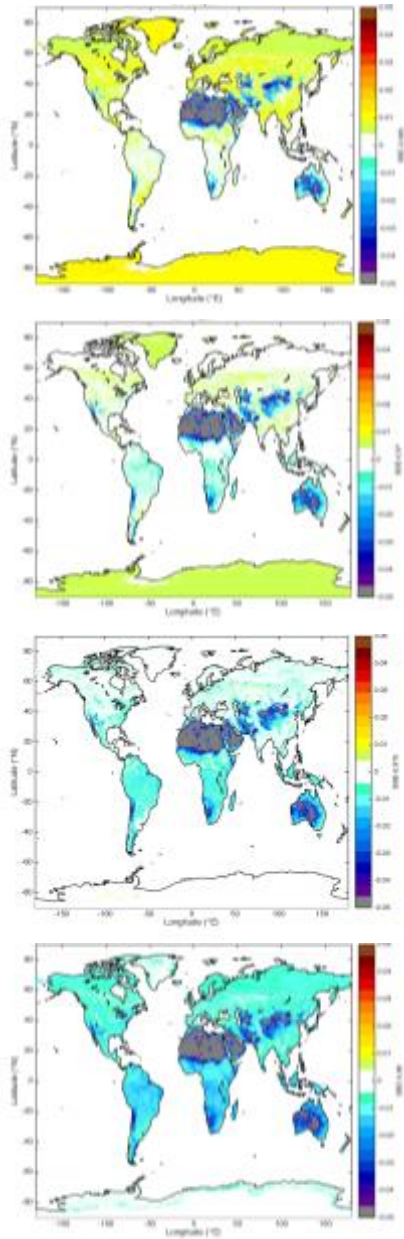


Figure 3. CAMEL 8.0-13.5 μm Jan 2007 BBE minus 0.965 (top), 0.970 (second from top), 0.975 (second from bottom), and 0.980 (bottom).

Monthly climatologies of CAMEL BBE over the years 2003 – 2015 for the 8.0-13.5 μm are calculated and shown for 4 months that represent different seasons in Figure 4.

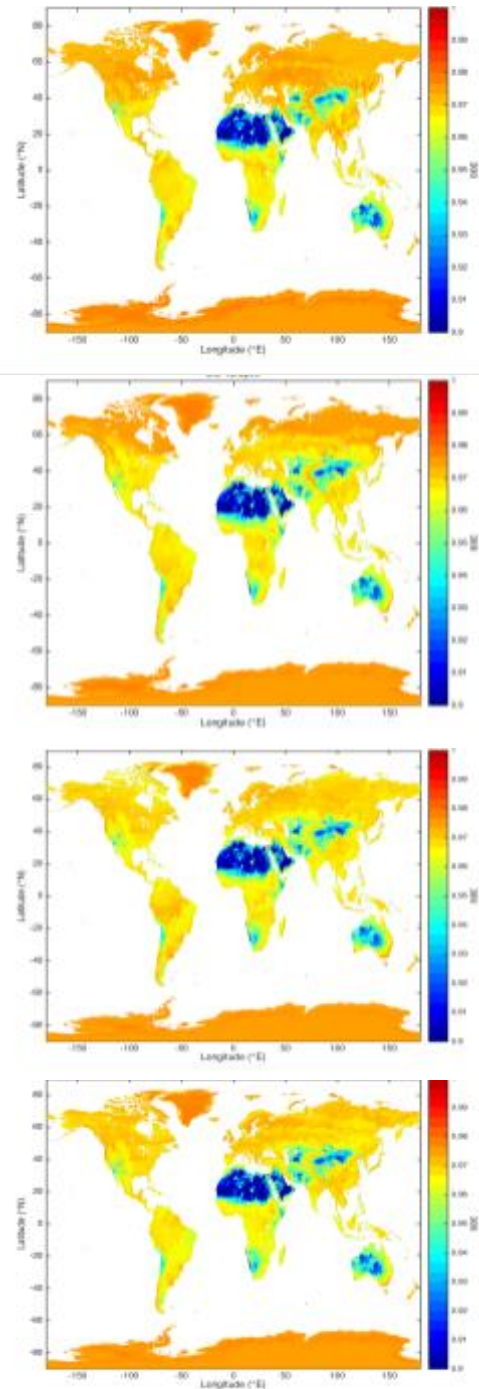


Figure 4. Monthly climatology of CAMEL 8.0-13.5 μm BBE over 2003 - 2015 for the month of January (top), April (second from top), July (second from bottom), and October (bottom).

To illustrate how the monthly CAMEL BBE changes from year to year, Figure 5 depicts January monthly CAMEL BBE minus climatology for the years of 2015 and 2003. Larger than one percent differences are seen between the single month and climatology BBE in various locations including south of the Sahara Desert, southeast of the Aral Sea, and numerous regions around northeastern and middle Asia such as the Himalayas, Gobi Desert, Plateau of Tibet and areas to the north. Of four seasonal months investigated (not shown), January is seen to have the largest differences from its climatology. Interestingly, it is common that the sign of this difference is reversed between 2015 and 2003, which could be due to a trend in BBE over the years, but may be more likely due to changes in the versions of data that are input into the CAMEL emissivity product.

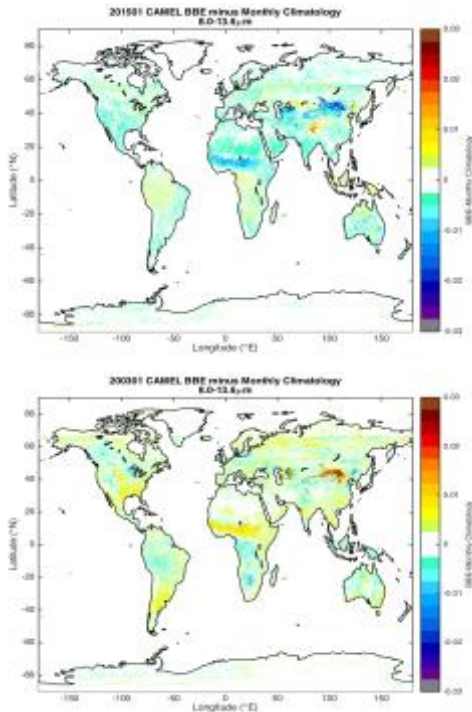


Figure 5. January CAMEL 8.0-13.5 μm BBE minus climatology for 2015 (top) and 2003 (bottom).

Variation of CAMEL broadband emissivity over time is shown in Fig. 6 as time series for the 8.0-13.5 micron band for the four case sites of Fig 1. Change over the years is not seen to be large, which is desired for such sites that are used for validation of the emissivity dataset. Mountainous regions experience larger changes from month to month—an example region in the Colorado Rocky Mountains experiences annual changes of ~ 0.02 in BBE (not shown).

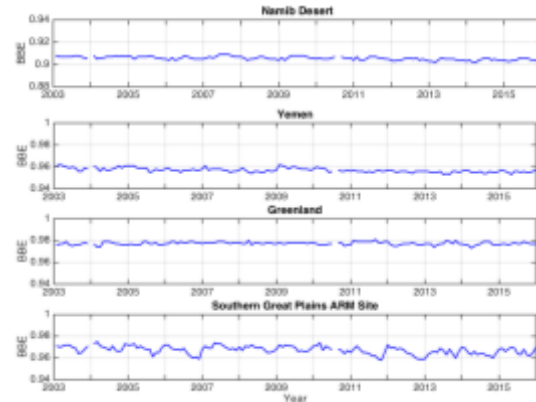


Figure 6. Time series of monthly 0.5x0.5 degree CAMEL 8.0-13.5 μm BBE for the 4 sites as in Figure 1.

4.2 BBE by Land Type and Climate Regime

To investigate how BBE changes with land type and climate regime, statistics are calculated over IGBP land cover classifications and Köppen-Geiger Climate Classification schemes. A map of IGBP land cover categories is shown in Fig. 7 (taken from Congalton et al. (2014)). In order to calculate the statistics, the IGBP categories and Köppen-Geiger schemes needed to be mapped to the CAMEL 0.05x0.05 degree resolution grid. Both the IGBP categories and Köppen-Geiger schemes were made available on 0.5x0.5 degree grids, so they simply needed to be gridded to the higher CAMEL resolution. Yearly updates of the IGBP land cover were available from 2002-2007, so the categories for year 2007 were used for IGBP statistics over all the years 2007-2015. For Köppen-Geiger schemes a single, present day representative map of categories was used for all years.

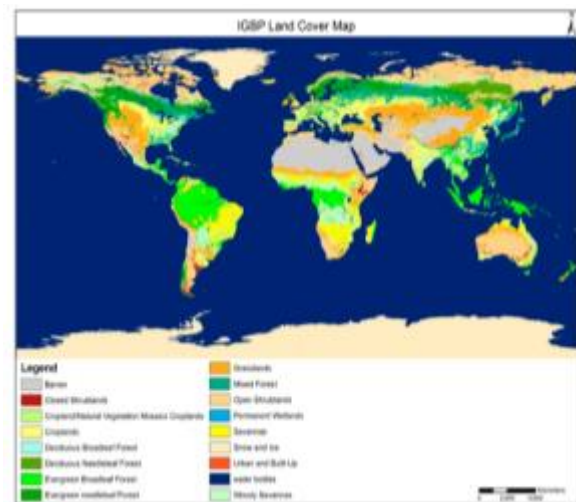


Figure 7. IGBP land cover categories. Taken from Congalton et al. (2014).

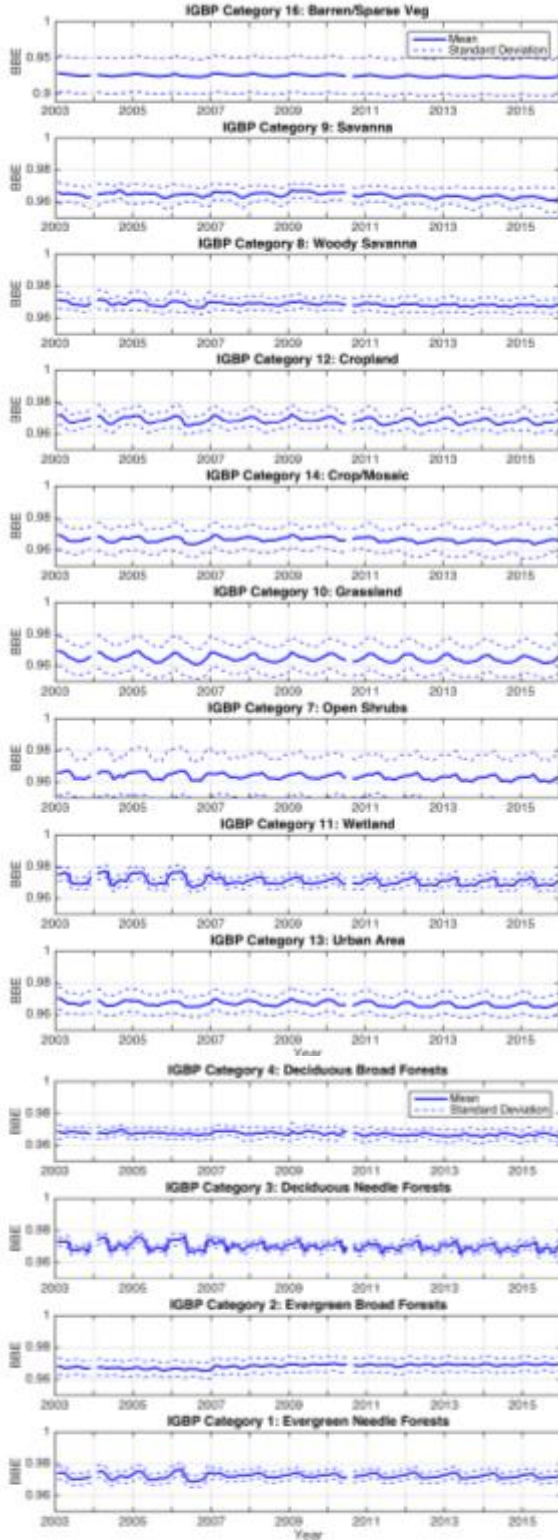


Figure 8. Time series of CAMEL 8.0-13.5 μm BBE statistics by IGBP land cover classifications. Note the y-axis limit is different for the top panel.

For each month and land cover category, the mean, μ , standard deviation, σ , and uncertainty of the mean, μ_{unc} , is calculated. Uncertainty of the mean is calculated as follows:

$$m_{unc} = \left(\frac{s}{\sqrt{N}} \right), \quad (2)$$

where N is the number of samples; however, the uncertainty is found to be negligible so is not shown in figures.

Time series of monthly mean 8.0-13.5 micron BBE overlaid with monthly mean \pm monthly standard deviations are shown for IGBP categories in Fig 8. Categories with higher changes in mean BBE throughout the year include grassland, cropland, open shrubs, wetland, and needle forests. Larger monthly standard deviations, which indicate the land cover types that are not as well represented by a single, constant BBE value, are seen for the barren/sparse vegetation, grassland, and open shrub categories.

Time series of statistics over the main Köppen-Geiger climates are shown in Fig 9. BBE averaged over the Köppen-Geiger Climate Classifications changes less over time than BBE averaged over the IGBP land types, likely due to the fact that the different climatic regimes do not as closely represent single BBE values. The arid climate's high monthly standard deviation suggests this climatic regime is a mixing of more diverse BBE values than the other regimes.

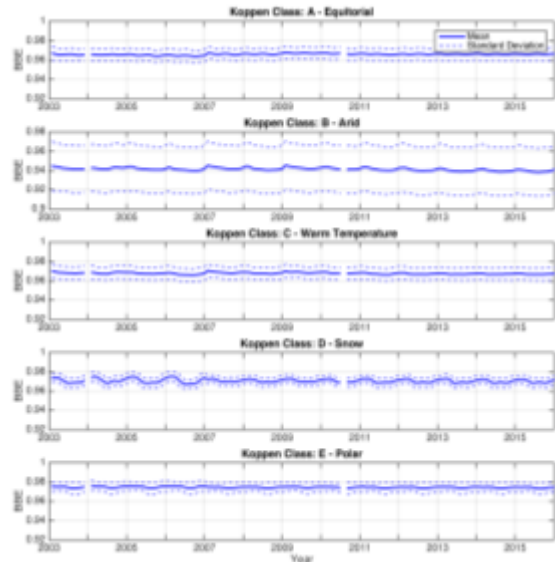


Figure 9. Time series of CAMEL 8.0-13.5 μm BBE statistics by the Köppen-Geiger Climate Classification scheme main climates.

5. CONCLUSIONS

This work presented and applied a method for obtaining surface broadband emissivity estimates from the recently released MEaSUREs CAMEL beta v0.6 emissivity dataset. In comparison to previous methods which are based upon regression techniques using satellite narrow band channels, this method takes advantage of the CAMEL high spectral resolution emissivity product and integrates equation (1) to obtain BBE estimates.

BBE calculations were performed for two wavelength ranges: 1) the full CAMEL 3.6-14.3 micron range and 2) the 8.0-13.5 micron range. The first range was used to take advantage of the full, available high spectral resolution CAMEL spectrum. The second range was selected based on work of previous studies (Ogawa and Schmugge, 2004; Cheng et al., 2013). Both Ogawa and Schmugge (2004) and Cheng et al. (2013) found that from various wavelength ranges studied, BBE over the 8.0-13.5 micron range was optimal for computing all wavelength LW net radiation, which is a key parameter in radiation models.

Differences of the monthly CAMEL BBE product from single, global constants were shown to illustrate the error from using single, constants over time and space to represent BBE in radiation models. Differences from 0.98, a constant which is known to be used in various models, revealed magnitudes greater than 0.05. Results for the example month included showed more appropriate constant values could be chosen for different months than 0.98.

Monthly climatologies over the full CAMEL record were presented. Statistics over IGBP land cover categories and Köppen-Geiger climates showed the potential of the CAMEL dataset to be used for developing BBE parameterizations for use in radiation type models.

Acknowledgments

We acknowledge the the NASA and USGS Land Processes Distributed Active Archive Center for providing MODIS skin temperature product and the Global Land Cover Facility for the MODIS IGBP land cover product. We also acknowledge the Institute for Veterinary Public Health for providing the Köppen-Geiger Climate Classification scheme data. This work was funded by grant number: 1498402.

References

Channan, S., K. Collins, and W. R. Emanuel. "Global mosaics of the standard MODIS land

cover type data." University of Maryland and the Pacific Northwest National Laboratory, College Park, Maryland, USA. 2014.

Cheng, Jie, et al. "Estimating the optimal broadband emissivity spectral range for calculating surface longwave net radiation." *IEEE Geoscience and Remote Sensing Letters* 10.2(2013): 401-405.

Cheng, Jie, et al. "A Comparative Study of Three Land Surface Broadband Emissivity Datasets from Satellite Data." *Remote Sensing* 6 (2014): 111-134, doi:10.3390/rs6010111.

Congalton et al. "Global Land Mapping: A review and uncertainty analysis." *Remote Sens.*, 6 (2014): 12070-12083.

Hulley, Glynn C., et al. "The ASTER Global Emissivity Dataset (ASTER GED): Mapping Earth's emissivity at 100 meter spatial scale." *Geophysical Research Letters* 42.19 (2015): 7966-7976.

Kottek, Markus, et al. "World map of the Köppen-Geiger climate classification updated." *Meteorologische Zeitschrift* 15.3 (2006): 259-263.

Ogawa, Kenta, et al. "Estimation of broadband land surface emissivity from multi-spectral thermal infrared remote sensing." *Agronomie* 22.6 (2002): 695-696.

Ogawa, Kenta, and Thomas Schmugge. "Mapping surface broadband emissivity of the Sahara Desert using ASTER and MODIS data." *Earth Interactions* 8.7 (2004): 1-14.

Ogawa, Kenta, Thomas Schmugge, and Shuidhi Rokugawa. "Estimating broadband emissivity of arid regions and its seasonal variations using thermal infrared remote sensing." *IEEE Transactions on Geoscience and Remote Sensing* 46.2 (2008): 334-343.

Seemann, Suzanne W., et al. "Development of a global infrared land surface emissivity database for application to clear sky sounding retrievals from multispectral satellite radiance measurements." *Journal of Applied Meteorology and Climatology* 47.1 (2008): 108-123.

Wilber, A. et al. *Surface Emissivity Maps for Use in Satellite Retrievals of Longwave Radiation*; NASA/TP-1999-209362; NASA Langley Research Center: Hampton, VA, USA, 1999. Available online: <http://techreports.larc.nasa.gov/1ts> (accessed on 08 August 2016).